

Expansion method for stationary states of quantum billiards

David L. Kaufman

Department of Physics, Bethel College, 300 East 27th Street, North Newton, Kansas 67117

Ioan Kosztin

The James Franck Institute, The University of Chicago, 5640 South Ellis Avenue, Chicago, Illinois 60637

Klaus Schulten^{a)}

Department of Physics, University of Illinois at Urbana-Champaign, 1110 West Green Street, Urbana, Illinois 61801

(Received 16 January 1998; accepted 6 June 1998)

A simple expansion method for numerically calculating the energy levels and the corresponding wave functions of a quantum particle in a two-dimensional infinite potential well with arbitrary shape (quantum billiard) is presented. The method permits the study of quantum billiards in an introductory quantum mechanics course. According to the method, wave functions inside the billiard are expressed in terms of an expansion of a complete set of orthonormal functions defined in a surrounding rectangle for which the Dirichlet boundary conditions apply, while approximating the billiard boundary by a potential energy step of a sufficiently large size. Numerical implementations of the method are described and applied to determine the energies and wave functions for quarter-circle, circle, and triangle billiards. Finally, the expansion method is applied to investigate the quantum signatures of chaos in a classically chaotic generic-triangle billiard.

© 1999 American Association of Physics Teachers.

I. INTRODUCTION

One of the most striking predictions of quantum mechanics is the *discreteness* of the energy spectrum of a microscopic particle whose motion is confined in space. The allowed values of energy for such a particle, together with the corresponding wave functions (i.e., *stationary states*), can be determined by solving the (time-independent) Schrödinger equation, subject to some properly chosen boundary conditions. Perhaps the simplest example in this respect is the problem of a particle in an infinite potential well. The particle is trapped inside the well, a simply connected region \mathcal{S} , where it can move freely. Since the Schrödinger equation for a free particle assumes the form of the well-known Helmholtz equation¹

$$(\nabla^2 + k^2)\psi(\mathbf{r}) = 0, \quad \mathbf{r} \in \mathcal{S}, \quad (1.1)$$

the problem of determining the stationary states of the particle in the infinite well amounts to the calculation of the eigenvalues and eigenfunctions as stated by Eq. (1.1) for Dirichlet (hard wall) boundary conditions along the boundary $\Gamma = \partial\mathcal{S}$ of the well, i.e.,

$$\psi(\mathbf{r})|_{\mathbf{r} \in \Gamma} = 0. \quad (1.2)$$

In Eq. (1.1) $k = \sqrt{2ME}/\hbar$ is the wave vector, where M , E (>0), and \hbar are the mass of the particle, the energy of the particle, measured from the bottom of the well, and Planck's constant divided by 2π , respectively.

In one dimension, Eq. (1.1) is the ordinary differential equation of the vibrating string, and the solution of the eigenvalue problem (1.1)–(1.2) is presented in all introductory quantum mechanics textbooks.¹ In two-dimension (2D), the degree of difficulty in solving the above eigenvalue problem depends on the actual shape of the infinite well. Hereafter, for obvious reasons, we shall refer to a particle in a 2D infinite potential well as a (quantum) billiard. When the shape of the billiard is highly regular, such as square, rect-

angular, or circular, then Eq. (1.1) can be solved by means of separation of variables. Thus the energy eigenvalues and eigenfunctions of the square and rectangle billiards can be expressed in terms of the results for the one-dimensional well. Furthermore, the square billiard is a good example to illustrate the concept of degeneracy of an energy level due to geometrical symmetries, whereas the rectangular billiard provides a first example for what is called “accidental” degeneracy (when the ratio of the edge lengths of the rectangle is a rational number), which does not originate from symmetry. The stationary states of a circle billiard² can also be determined analytically by employing plane-polar coordinates in Eq. (1.1). For the radial part of the wave function one obtains the differential equation of the Bessel functions and one finds that the corresponding energy levels can be expressed in terms of the zeros of the integer Bessel functions. The study of the angular part of the wave function for a circle billiard provides the opportunity to introduce the quantum mechanical description of the angular momentum and to relate the degeneracy in the energy spectrum to the rotational symmetry with respect to the symmetry axis of the system.

The problem of determining the stationary states of a generic quantum billiard, with arbitrary shape, is not covered in quantum mechanics textbooks. Presumably, the main reason for this is that a generic quantum billiard cannot be solved analytically and apparently a tedious and costly numerical calculation would benefit the student too little. However, quantum billiards have recently attracted much interest in quantum physics and electronics such that an introduction to these quantum systems in modern physics is now desirable. Advances in crystal growth and lithographic techniques have made it possible to produce very small and clean devices, known as *nanodevices*.³ The electrons in such devices, through gate voltages, are confined to one or two spatial

dimensions. At sufficiently low temperatures, a 2D nanodevice in which the electrons are confined to a finite 2D domain of submicron size should be regarded as an experimental realization of a quantum billiard. Under these conditions the motion of electrons inside the device is ballistic, i.e., the electrons are scattered mainly by the device boundary and not by impurities or other electrons. The behavior of such a nanodevice is governed by single-particle physics and, accordingly, can be described by solving the time-independent Schrödinger equation for a particle in a 2D infinite potential well, i.e., by solving the eigenvalue problem (1.1)–(1.2). Thus quantum billiards can be regarded as models of nanodevices which play an important role in today’s semiconductor industry.³ It should be noted that the theoretical predictions of quantum mechanics for a quantum billiard can be tested experimentally by using scanning tunneling microscopy.³

The study of quantum billiards is also of great interest in the relatively new field of *quantum chaos*.⁴ Generic billiards are one of the simplest examples of conservative dynamical systems with chaotic classical trajectories. In general, chaos refers to the exponential sensitivity of a classical phase space trajectory on the initial conditions. It is known that integrable systems (which have the same number of constants of motion as their dimension), such as billiards with regular shape, are nonchaotic, whereas nonintegrable systems (with fewer constants of motion than their dimensionality), such as generic billiards, are chaotic.⁵ In billiards the chaotic behavior is caused by the irregularities of the boundary and not by the complexity of the interaction in the system (e.g., scattering of the particle from randomly distributed impurities). Since the concept of “phase space trajectory” loses its meaning in quantum mechanics, one can naturally ask oneself what is the quantum mechanical analogue of (classical) chaos, or more precisely, is there any detectable difference between the behavior of a quantum system with chaotic and nonchaotic classical limits, respectively. The answer to these questions should be sought in the statistics of the energy levels of the billiard and in the morphology of the corresponding wave functions.

Although the stationary states of a generic billiard can be computed only numerically, the analogy between the Schrödinger and Helmholtz equations allows us to compare the obtained numerical results with the experimentally determined eigenmodes of a vibrating membrane, or the resonant modes of the oscillating electromagnetic field in a resonant cavity, of the same shape as the billiard. In fact, this analogy has been exploited by several authors who employed microwave cavities in order to measure directly, with high accuracy, both the eigenvalues and eigenfunctions in model billiard geometries.⁶

The aim of this article is to present a simple, yet quite general and powerful, numerical method, referred to as the *expansion method* (EM), for calculating the stationary states of quantum billiards. This method is conceptually simple and should be accessible to students interested in quantum mechanics. The EM together with its computer implementation, e.g., as a MATHEMATICA notebook,⁷ may also be of interest for those engaged in teaching introductory quantum mechanics.

This article is structured as follows. The formulation of the EM, along with its computer implementation, is given in Sec. II. In Sec. III the EM is applied to calculate the stationary states of three integrable billiards (quarter-circle, circle,

and equilateral-triangle) and the calculated values of the energy levels are compared with the corresponding exact analytical results. Next, in Sec. IV, the results of similar calculations for several chaotic billiards (isosceles and generic triangles) are presented. In Sec. V the energy level spacing distributions corresponding to the studied quantum billiards are compared with the theoretical predictions of the random matrix theory⁸ (RMT) and used to distinguish billiards which are classically integrable from those which are chaotic. Finally, Sec. VI presents conclusions.

II. THE EXPANSION METHOD

There exist several efficient numerical methods for calculating the energy spectrum of a generic quantum billiard (a classification of these methods is provided in Ref. 9), but all of them have certain shortcomings which make them unsuitable for the study of quantum billiards in an introductory quantum mechanics course. The expansion method (EM), we describe next, is simple, intuitive, quite general, and powerful enough to allow us to determine simultaneously both the energy levels and the corresponding wave functions of a quantum billiard.

Consider a particle of mass M moving in a 2D infinite potential well,

$$V(\mathbf{r}) = \begin{cases} 0 & \text{if } \mathbf{r} \in \mathcal{D} \\ \infty & \text{otherwise} \end{cases} \quad (2.1)$$

The corresponding stationary states are given by the eigenvalues and eigenfunctions of the time-independent Schrödinger equation

$$\hat{H}\psi_n(\mathbf{r}) = \left[-\frac{\hbar^2}{2M} \nabla^2 + V(\mathbf{r}) \right] \psi_n(\mathbf{r}) = E_n \psi_n(\mathbf{r}). \quad (2.2)$$

Since the potential energy is infinitely large outside the domain \mathcal{D} , the wave functions $\psi_n(\mathbf{r})$ must obey the Dirichlet boundary condition (1.2). By introducing the wave vector

$$k_n = \sqrt{\frac{2ME_n}{\hbar^2}}, \quad (2.3)$$

Eqs. (2.2)–(2.1) yield the eigenvalue problem (1.1)–(1.2).

The EM is founded on the approximation of the potential energy (2.1) through

$$\tilde{V}(\mathbf{r}) = \begin{cases} 0 & \text{if } \mathbf{r} \in \text{I} \equiv \mathcal{D} \\ V_0 & \text{if } \mathbf{r} \in \text{II} \\ \infty & \text{if } \mathbf{r} \in \text{III} \end{cases}, \quad (2.4)$$

where V_0 is a properly chosen large constant; domains I, II, III are specified in Fig. 1. Approximation (2.4) amounts to fitting the generic billiard inside a rectangular infinite potential well of edge lengths a_1 and a_2 , and then replacing the infinite potential energy in region II (determined by what remains from the rectangular domain after removing \mathcal{D} , i.e., region I; see Fig. 1) by a sufficiently large, but finite, value V_0 . Since $\lim_{V_0 \rightarrow \infty} \tilde{V}(\mathbf{r}) = V(\mathbf{r})$, one expects that both $V(\mathbf{r})$ and $\tilde{V}(\mathbf{r})$ will lead approximately to the same stationary states as long as the associated energies are less than V_0 .

Approximation (2.4) also replaces boundary condition (1.2) by

$$\psi(\mathbf{r})|_{\mathbf{r} \in \bar{\text{I}}} = 0, \quad (2.5)$$

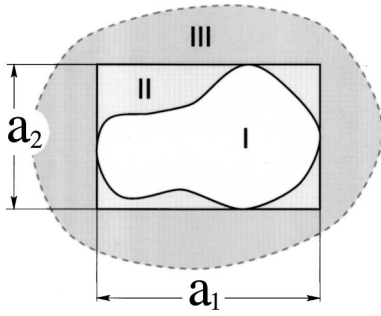


Fig. 1. Generic 2D billiard (I) fitted in a rectangular domain (II). The potential energy vanishes in region I, it has a finite value V_0 in region II, and it is infinitely large in the rest of the plane (region III).

where $\tilde{\Gamma}$ is the boundary of a rectangular well. This modification of the boundary condition has two important implications. First, the corresponding stationary state wave functions $\psi_n(\mathbf{r})$ do not vanish identically in region II (i.e., between Γ and $\tilde{\Gamma}$) but, for $E_n \ll V_0$, they assume a very small value (controlled by V_0) in this region. Second, the functions $\psi_n(\mathbf{r})$ can be expressed as

$$\psi(\mathbf{r}) = \sum_m c_m \phi_m(\mathbf{r}), \quad (2.6)$$

where c_m are expansion coefficients to be determined; $\phi_m(\mathbf{r})$ are the energy eigenfunctions corresponding to a particle in the rectangular infinite potential well, i.e.,

$$\begin{aligned} \phi_m(\mathbf{r}) &\equiv \phi_{m_1, m_2}(x_1, x_2) \\ &= \sqrt{\frac{2}{a_1}} \sin\left(\frac{\pi}{a_1} m_1 x_1\right) \sqrt{\frac{2}{a_2}} \sin\left(\frac{\pi}{a_2} m_2 x_2\right). \end{aligned} \quad (2.7)$$

The functions $\phi_m(\mathbf{r})$ form a complete set of orthonormal functions. In Eq. (2.7) $x_{1,2}$ are Cartesian coordinates oriented along two perpendicular edges of the rectangle of lengths $a_{1,2}$, and $m = (m_1, m_2)$ are doublets of positive integers. The orthonormality condition of the functions $\phi_m(\mathbf{r})$ reads

$$\int d\mathbf{r} \phi_n(\mathbf{r}) \phi_m(\mathbf{r}) = \delta_{nm}, \quad (2.8)$$

where the Kronecker-delta δ_{nm} is equal to one for $n = m$ and zero otherwise. The possibility to employ the convenient expansions (2.6) and (2.7) is the reason why approximation (2.4) has been introduced. The price one needs to pay is that the resulting wave functions do not vanish exactly in region II. However, by choosing V_0 large enough this error can be kept small as demonstrated below.

Inserting Eq. (2.6) into the Schrödinger equation (2.2), with V replaced by \tilde{V} , multiplying the result from the left by $\phi_n(\mathbf{r})$, and integrating with respect to the position vector, one arrives at the matrix eigenvalue equation

$$\sum_m (H_{nm} - E \delta_{nm}) c_m = 0. \quad (2.9)$$

In deriving Eq. (2.9) we have used the orthonormality condition (2.8), and defined the matrix elements of the Hamiltonian as

$$H_{nm} = \int d^2\mathbf{r} \phi_n(\mathbf{r}) \hat{H} \phi_m(\mathbf{r}). \quad (2.10)$$

Using the Hamiltonian $\hat{H} = -(\hbar^2/2M)\nabla^2 + \tilde{V}(\mathbf{r})$ together with (2.4) and (2.7) one can evaluate these matrix elements and obtain

$$H_{nm} = \frac{\pi^2 \hbar^2}{2m} \left[\left(\frac{m_1}{a_1}\right)^2 + \left(\frac{m_2}{a_2}\right)^2 \right] \delta_{nm} + V_0 v_{nm}. \quad (2.11)$$

Here we used the notations: $m = (m_1, m_2)$, and

$$v_{nm} = \int_{\text{II}} d^2\mathbf{r} \phi_n(\mathbf{r}) \phi_m(\mathbf{r}), \quad (2.12)$$

where $\int_{\text{II}} d^2\mathbf{r} \cdots$ denotes integration over region II (see Fig. 1).

The (approximate) energy levels E of the quantum billiard are given by the condition that the homogeneous matrix equation (2.9) has nontrivial solutions, i.e., the allowed energy levels are those which obey

$$\det|H_{nm} - E \delta_{nm}| = 0. \quad (2.13)$$

The corresponding energy values are a discrete set E_n , $n = 1, 2, \dots$. We assume the ordering $E_n < E_m$ for $n < m$. Once the energy eigenvalues E_n are determined, they are inserted in (2.9) and the resulting sets of linear equations have to be solved for the unknown expansion coefficient $c_m^{(n)}$, which provide the desired wave functions $\psi_n(\mathbf{r}) = \sum_m c_m^{(n)} \phi_m(\mathbf{r})$ [cf. Eq. (2.6)].

In practice, the application of the EM requires a second approximation, since in expansion (2.6) one can retain only a finite number of M_0 terms. This implies that the Hamiltonian matrix H_{nm} is truncated, and that the approximate stationary states of the billiard are described by the eigenvalues and the eigenvectors of this truncated $M_0 \times M_0$ matrix. The diagonalization of H_{nm} yields as many states as the dimension M_0 of the matrix. However, due to the truncation process only a fraction of the obtained states with the lowest energies can be trusted. In fact, it must hold $E_1, E_2, \dots \ll V_0$ and only m_0 states with $m_0 \ll M_0$ can be used. In principle, by using sufficiently large M_0 and V_0 values, one can determine accurately an arbitrarily large number m_0 of stationary states. In practice, however, by increasing the values of M_0 and V_0 the required computational resources (both CPU time and memory) proliferate exponentially and, therefore, the total number of stationary states which can be obtained by using the EM method are actually limited.

Numerical algorithm—The formulation of a numerical algorithm based on the EM is straightforward. The steps of the algorithm are the following.

- (1) Define proper energy and length units. It is convenient to chose as energy unit $\hbar^2/2Ma_1^2$, and as length unit a_1 .
- (2) Define the shape of the billiard (Γ) and calculate the edge lengths a_1 and a_2 of a rectangle which encompasses Γ completely.
- (3) Chose proper values for M_0 and V_0 .
- (4) Evaluate and save the symmetric matrix $v_{n,m}$, $n, m \leq M_0$, by calculating *analytically* the integrals (2.12). If the shape of the billiard is such that these integrals cannot be evaluated analytically then the efficiency of the

Table I. Comparison between the exact wave vectors k_n and the ones computed numerically by using the expansion method (EM) corresponding to the first sixteen stationary states for: (1) quarter-circle, (2) full-circle, and (3) equilateral-triangle billiards. The corresponding energy eigenvalues E_n , in units of $2\pi\hbar^2/2M\mathcal{A}$, are also given.

State n	1) Quarter Circle				2) Circle				3) Equilateral Triangle			
	k_n (EM)	k_n (Exact)	Δk_n ($10^{-2}\%$)	E_n $\left(\frac{2\pi\hbar^2}{M\mathcal{A}}\right)$	k_n (EM)	k_n (exact)	Δk_n (%)	E_n $\left(\frac{2\pi\hbar^2}{M\mathcal{A}}\right)$	k_n (EM)	k_n (exact)	Δk_n ($10^{-2}\%$)	E_n $\left(\frac{2\pi\hbar^2}{M\mathcal{A}}\right)$
1	5.1351	5.1351	0.9	1.648	2.4002	2.4048	0.19	0.360	7.2547	7.2551	0.66	1.815
2	7.5918	7.5883	4.5	3.602	3.8226	3.8317	0.23	0.913	11.0690	11.0824	12.11	4.221
3	8.4165	8.4172	0.7	4.427	3.8226	3.8317	0.23	0.913	11.0856	11.0824	2.81	4.234
4	9.9375	9.9361	1.4	6.172	5.1213	5.1356	0.27	1.639	14.5135	14.5103	2.19	7.258
5	11.0702	11.0647	4.9	7.659	5.1273	5.1356	0.16	1.643	15.0888	15.1028	9.31	7.845
6	11.6193	11.6198	0.4	8.438	5.5099	5.5200	0.18	1.897	15.1077	15.1028	3.21	7.864
7	12.2279	12.2251	2.3	9.345	6.3679	6.3801	0.19	2.534	18.2398	18.2585	10.20	11.463
8	13.5918	13.5893	1.9	11.546	6.3679	6.3801	0.19	2.534	18.2737	18.2585	8.36	11.506
9	14.3804	14.3725	5.5	12.924	6.9997	7.0155	0.22	3.062	19.1826	19.1954	6.65	12.679
10	14.4781	14.4755	1.8	13.100	6.9997	7.0155	0.22	3.062	19.2053	19.1954	5.15	12.709
11	14.7960	14.7950	0.0	13.682	7.5699	7.5883	0.24	3.581	21.7810	21.7655	7.10	16.347
12	16.0425	16.0378	3.0	16.085	7.5754	7.5883	0.17	3.586	22.1520	22.1649	5.82	16.908
13	16.7016	16.6982	2.0	17.433	8.3950	8.4172	0.26	4.404	22.1859	22.1649	9.43	16.960
14	17.0080	17.0038	2.4	18.079	8.4047	8.4172	0.14	4.414	23.3125	23.3221	4.12	18.727
15	17.6269	17.6159	6.2	19.419	8.6391	8.6537	0.16	4.664	23.3430	23.3221	8.94	18.776
16	17.9609	17.9598	0.6	20.162	8.7551	8.7714	0.18	4.790	25.4634	25.4794	6.27	22.342

EM is jeopardized due to the required large number of numerical integrations involving highly oscillatory integrands.

- (5) Evaluate the Hamiltonian matrix H_{nm} by using Eq. (2.10).
- (6) Find the eigenvalues E_n (energy levels) and the corresponding eigenvectors $c_m^{(n)}$ of the Hamiltonian matrix.
- (7) Determine the wave functions $\psi_n(\mathbf{r})$ according to Eq. (2.6).

We have implemented the above algorithm as a MATHEMATICA3.0 notebook. The actual code can be made extremely compact by employing the excellent built-in functions that MATHEMATICA3.0 offers, together with the standard LinearAlgebra`MatrixManipulation` package. For example, once the symmetric matrix H_{nm} is determined, the single command Eigensystem [Hnm] returns both the eigenvalues and the eigenvectors of the truncated Hamiltonian. Also, the obtained wave functions can be conveniently visualized as three-dimensional (3D) plots (with the Plot3D command) or density plots (by employing the DensityPlot MATHEMATICA command).

In general the most time-consuming part of the algorithm is the evaluation of the matrix v_{nm} . Note, however, that for a given billiard this matrix should be evaluated only once and it is a good idea to save it on the hard disk. The already existing matrix elements need not be reevaluated even if one increases the value of the truncation constant M_0 in order, e.g., to determine more energy levels.

The approximations connected with the EM, i.e., the truncation size M_0 of the matrix H_{nm} and the magnitude of V_0 , need to be carefully explored. M_0 should be large enough so that the truncated series (2.6) will accurately describe any desired stationary state. The higher the energy of the desired state, the more basis functions ϕ_m need to be included in the

expansion. The reason is that higher energy wave functions will have faster spatial oscillations than lower energy wave functions. A good rule of thumb in choosing a value for M_0 is to take the kinetic energy corresponding to $\phi_{M_0}(\mathbf{r})$ to be about 10 times larger than the highest desired energy level E_n ; a good choice for V_0 is about 10 times E_n . Note that although the size of V_0 does not effect the CPU time, too large a value of this quantity results in erroneous eigenvalues due to internal over/underflow errors.

III. INTEGRABLE SYSTEMS

First we apply the EM to calculate the stationary states of three examples of integrable billiards (quarter-circle, circle, and equilateral-triangle) for which analytical solutions are available. The wave vectors k_n corresponding to the first sixteen stationary states for these systems, which have been calculated numerically by employing the EM, are listed (the first column) and compared with the corresponding exact analytical results (the second column) in Table I. The agreement between the numerical and analytical results is extremely good, as indicated by the small relative error Δk_n (the third column). Furthermore, in Table I we also list the energies E_n of the considered stationary states (the fourth column) in units $2\pi\hbar^2/2M\mathcal{A}$, which allows us to compare the corresponding energy eigenvalues of billiards which have the same area \mathcal{A} but different shapes. As intuitively expected, the circle billiard has the smallest ground state energy, followed by the quarter-circle and the equilateral-triangle billiards.

A. Quarter-circle billiard

First we consider a quantum billiard, the boundary Γ of which is a quarter of a circle with unit radius. Expressing

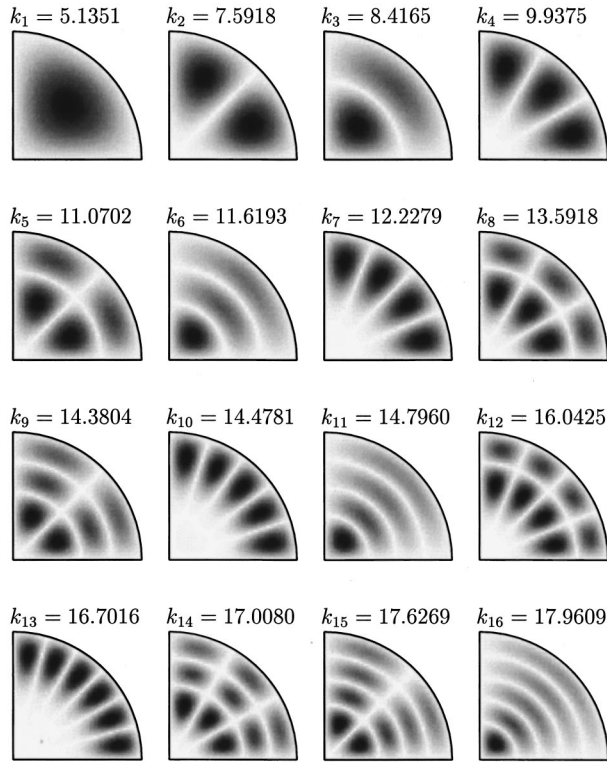


Fig. 2. Density plot of $|\psi(\mathbf{r})|$ corresponding to the first sixteen stationary states (of lowest energy) for the quarter-circle billiard. The values of the corresponding wave vectors k_n are listed above each graph, in units specified in the text.

$E_n = \hbar^2 k_n^2 / 2M$, the wave vectors k_n are given by the zeros of the even-integer Bessel functions,¹ i.e., $J_{2m}(k_n) = 0$.

To employ the EM, we fit this billiard in a unit square, i.e., $a_1 = a_2 = 1$. The matrix elements (2.12), in this case, are given by

$$v_{nm} = 4 \int_0^1 dx_1 \sin(\pi n_1 x_1) \sin(\pi m_1 x_1) \times \int_{\sqrt{1-x_1^2}}^1 dx_2 \sin(\pi n_2 x_2) \sin(\pi m_2 x_2). \quad (3.1)$$

The latter integral can be evaluated analytically. The first fifty energy values resulting from the EM with $M_0 = 400$ and $V_0 = 50\,000$ are within 0.13% of the exact values. Density plots of the absolute value $|\psi_n(\mathbf{r})|$ of the wave function for the first sixteen stationary states are provided in Fig. 2.

B. Circle billiard

Next, we consider a full-circle billiard of unit radius centered about the origin. Analytical solutions for this system are well known.^{1,2} The energy eigenvalues are $E_n = \hbar^2 k_n^2 / 2M$, where the k_n values are given by the zeros of the integer Bessel functions of the first kind: $J_m(k_n) = 0$.

To employ the EM, we fit the billiard in a square with $a_1 = a_2 = 2$. Because the origin of the coordinate system is chosen in the center of the square, the corresponding basis functions are given by (2.7) in which $x_{1,2}$ are shifted by unity. The matrix elements v_{nm} are

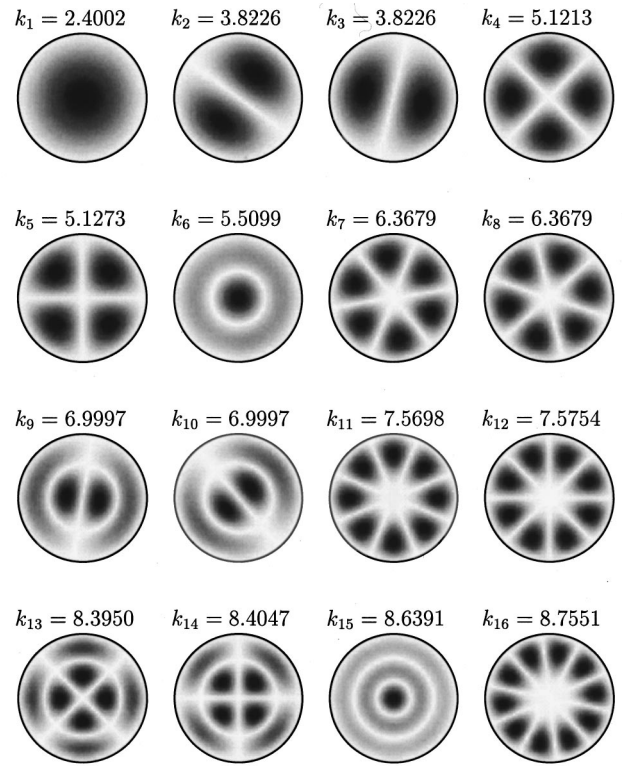


Fig. 3. Density plot of $|\psi_n(\mathbf{r})|$, $n = 1, \dots, 16$, for the circle billiard.

$$v_{nm} = \int_{-1}^1 dx_1 \int_{-1}^1 dx_2 \phi_n(x_1, x_2) \phi_m(x_1, x_2) - \int_{-1}^1 dx_1 \int_{-\sqrt{1-x_1^2}}^{\sqrt{1-x_1^2}} dx_2 \phi_n(x_1, x_2) \phi_m(x_1, x_2), \quad (3.2)$$

and, again, can be evaluated analytically.

In Table I the numerically calculated k_n 's, for the same values of M_0 and V_0 as above are compared with the exact values. Most of the energy levels, namely those with nonzero angular momentum, are doubly degenerate. Density plots for the first sixteen wave functions are shown in Fig. 3.

C. Equilateral-triangle billiard

The equilateral-triangle billiard is also integrable. The energy spectrum, in units $\hbar^2 / 2M a^2$, where a is the edge length, is given by¹⁰

$$E_n \equiv E_{pq} = \left(\frac{4\pi}{3} \right)^2 (p^2 + q^2 - pq), \quad 1 \leq q \leq p/2, \quad (3.3)$$

where p and q are positive integers. All the states are degenerate, except those with $p = 2q$.

The EM can be efficiently applied to triangle billiards because the matrix elements v_{nm} can be evaluated analytically. We fit the triangle inside a rectangle with $a_1 = 1$ and $a_2 = l$, l being the height of the triangle, which in the general case can be expressed in terms of two acute angles α_1 and α_2 . If one defines $\beta_i = \tan \alpha_i$, $i = 1, 2$, the vertices of the triangle have the coordinates $(0, 0)$, $(1, 0)$, and (x_b, l) , where

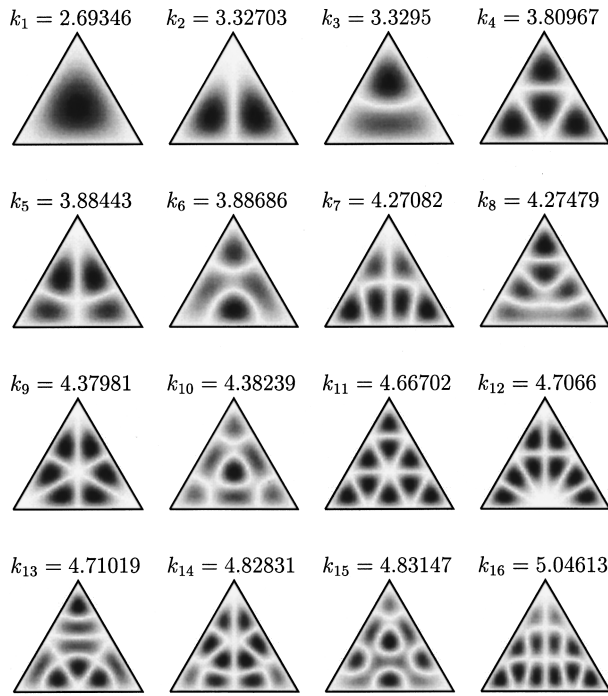


Fig. 4. Density plot of $|\psi_n(\mathbf{r})|$, $n = 1, \dots, 16$, for the equilateral-triangle billiard.

$$l = \frac{\beta_1 \beta_2}{\beta_1 + \beta_2}, \quad x_b = \frac{\beta_1}{\beta_1 + \beta_2}. \quad (3.4)$$

For an equilateral triangle $\alpha_1 = \alpha_2 = 60^\circ$, $l = \sqrt{3}/2$, and $x_b = 1/2$. The matrix elements v_{nm} are in this case

$$v_{nm} = \int_0^{x_b} dx_1 \int_{\beta_1 x_1}^l dx_2 \left\{ \cos[\pi(n_1 - m_1)x_1] - \cos[\pi(n_1 + m_1)x_1] \right\} \left\{ \cos\left[\frac{\pi}{l}(n_2 - m_2)x_2\right] - \cos\left[\frac{\pi}{l}(n_2 + m_2)x_2\right] \right\} + \int_{x_b}^1 dx_1 \int_{\beta_2(1-x_1)}^l dx_2 \left\{ \cos[\pi(n_1 - m_1)x_1] - \cos[\pi(n_1 + m_1)x_1] \right\} \left\{ \cos\left[\frac{\pi}{l}(n_2 - m_2)x_2\right] - \cos\left[\frac{\pi}{l}(n_2 + m_2)x_2\right] \right\}. \quad (3.5)$$

The first sixteen stationary states of an equilateral-triangle billiard are presented through their wave vectors k_n and wave functions in Fig. 4. One can see that the EM furnishes wave functions which decay to zero toward the edge of the triangle. The energy values indicate that the threefold symmetry has one-dimensional and two-dimensional representations,¹¹ i.e., there exist nondegenerate states and pairwise degenerate states. Due to the approximative character of the EM, the latter degeneracies are slightly broken with errors below 1%. Only 3 of the states shown, namely 1, 4, and 11, are nondegenerate, the corresponding wave functions exhibiting the threefold symmetry of the tri-

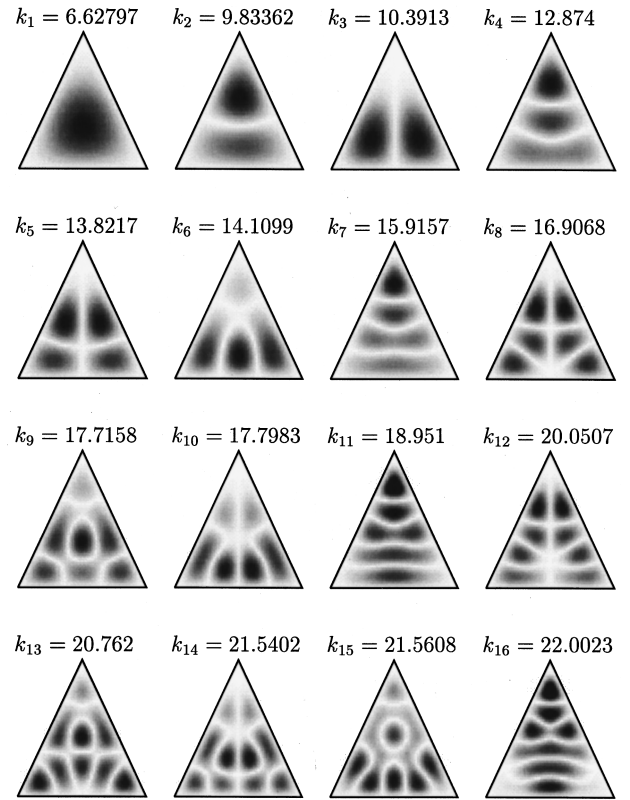


Fig. 5. Density plot of $|\psi_n(\mathbf{r})|$, $n = 1, \dots, 16$, for an isosceles-triangle billiard with $\alpha = \beta = 65^\circ$.

angle (see Fig. 4). The doubly degenerate states are presented through wave functions which do not exhibit the full symmetry of the equilateral triangle, but can be superimposed to be symmetric, in which case complex amplitudes are needed.

The wave functions in Fig. 4 reflect the well-known principle that increases in energy are accompanied by an increase in the number of nodal lines. For example, the nondegenerate states 1, 4, and 11 have, respectively, no nodal line, a nodal triangle (three lines), and three nodal triangles (nine nodal lines, two of which are oriented such that they form a single long line). Similarly, the first two pairs of nondegenerate states, (2,3) and (5,6), are characterized through one and through two nodal lines, respectively.

IV. CHAOTIC SYSTEMS

A. Isosceles-triangle billiard

Figure 5 presents the first sixteen stationary states (energies and wave functions) of the isosceles triangle with $\alpha_1 = \alpha_2 = 65^\circ$. In this case the double degeneracies, which arise in the equilateral triangle, are broken since the mirror symmetry of the isosceles triangles has only one-dimensional representations. One can relate quite well the states of the isosceles triangle to those of the equilateral triangle, in particular for the double-degenerate equilateral triangle states. In the case of state 4 one can discern that the wave function of this state evolves from that of state 4 of the equilateral case through a merging of the wave function minima in the two bottom corners. Similarly, state 11 of the isosceles triangle evolves through merging of wave function maxima (minima) of state 11 of the equilateral triangle. This ‘‘morphological’’ view of the wave functions in Fig. 5 emphasizes

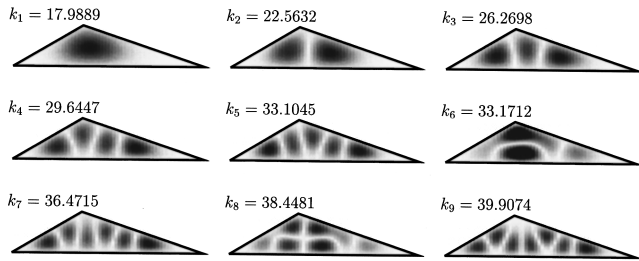


Fig. 6. Density plot of $|\psi_n(\mathbf{r})|$, $n = 1, \dots, 9$, for a generic-triangle billiard with $\alpha = 30.73^\circ$, and $\beta = 18.7^\circ$.

that the wave functions in the triangle depend sensitively on the triangle shape. One can readily imagine how a continuous change of the shape of the triangle “morphes” wave functions. What is not obvious is that continuous changes of the shape of the triangle can lead to new wave functions in cases when nodal lines merge with the triangle perimeter or detract from the triangle perimeter. These situations, which arise only in generic triangles, have been termed “diabolic points” in Ref. 10 and will be investigated now.

B. Generic-triangle billiard

In Ref. 10 the authors present several generic triangles in which the quantum states exhibit “diabolic points,” i.e., points of “accidental” degeneracy. Two of the triangles discussed by these authors are presented below together with the wave functions and energies of the first nine stationary states.

The first triangle we consider has angles 30.73° , 18.70° , and 130.57° . For this triangle one can discern in Fig. 6 a near degeneracy between states 5 and 6 (see energy values) corresponding to a diabolic point. The reader should note that the numerical approximation associated with the expansion method precludes exact degeneracies. Inspection of the wave functions of the first seven states of the triangle shows immediately that the wave functions of state 1, 2, 3, 4, 5, 7 follow the expected progression of an increasing number of maxima and minima, namely 1, 2, 3, 4, 5, and 6, respectively. State 6, however, sports solely three maxima (minima), one of the main characteristics of the wave function being a long squeezed feature, a “banana.”

The second triangle with angles 55.30° , 39.72° , and 84.98° , exhibits a similar scenario. The energy values shown in Fig. 7 exhibit a near degeneracy of states 6 and 7 corresponding to a “diabolic point.” The wave function of state 7 disrupts the progression of nodal lines and wave function maxima (minima) again: State 6 has a wave function with four connected regions without sign change, state 8 a wave function with five such regions, whereas state 7 has a wave function with only three such regions.

V. ENERGY LEVEL STATISTICS

One characteristic which distinguishes the spectra of integrable systems (e.g., quarter-, full-circle, and equilateral-triangle billiards) from chaotic ones (e.g., isosceles- and generic-triangle billiards) is the so-called *energy level spacing distribution*⁹ $P(s)$. By definition, $P(s)ds$ represents the probability that, given an energy level at E , the nearest-neighbor energy level is located in the interval ds about $E + s$. According to *random matrix theory* (RMT),^{8,4} appli-

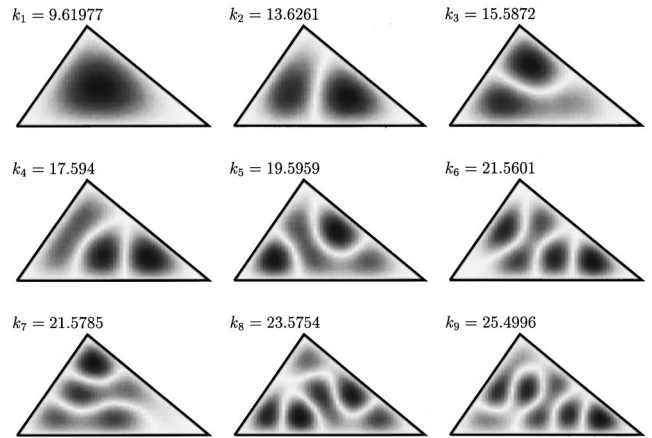


Fig. 7. Density plot of $|\psi_n(\mathbf{r})|$, $n = 1, \dots, 9$, for a generic-triangle billiard with $\alpha = 55.3^\circ$ and $\beta = 39.72^\circ$.

cable due to a quasirandom character of the Hamiltonian matrix H_{nm} , integrable systems are described by the Poisson distribution with

$$P_0(s) = e^{-s}. \quad (5.1)$$

The energy levels of classically chaotic systems, which do not break time reversal symmetry (e.g., the generic triangle without geometrical symmetries), form a *Gaussian orthogonal ensemble* (GOE) with

$$P_{\text{GOE}}(s) = \frac{\pi}{2} s \exp\left(-\frac{\pi s^2}{4}\right). \quad (5.2)$$

Poisson and GOE distributions are distinguished most clearly near $s=0$, since $P_0(0)=1$ [maximum of $P_0(s)$] and $P_{\text{GOE}}(0)=0$ [minimum of $P_{\text{GOE}}(s)$]; neighboring energy levels are likely to attract each other in the case of integrable systems, while in chaotic systems neighboring energy levels are likely to repel each other. In what follows we demonstrate that the level spacing distributions evaluated by means of the expansion method for the quarter-circle, circle, and triangle indeed obey these characteristics. For this purpose we evaluate $P(s)$ by using several hundred of the lowest energy levels calculated numerically by employing the expansion method.

First, one needs to make sure that the energy levels which enter in the determination of $P(s)$ are accurate. For the circle billiard this can be accomplished by comparing the EM results with the available exact energy eigenvalues. For the triangle billiard, where the exact energy eigenvalues are not known, one can check the correctness of EM energies through comparison with the *energy staircase function* $N(E)$ (which gives the number of quantum states with energy less than or equal to E) with the corresponding *Weyl-type formula*⁴

$$\langle N(E) \rangle = \frac{1}{4\pi} (\mathcal{A}E - \mathcal{L}\sqrt{E} + \mathcal{C}), \quad (5.3)$$

where \mathcal{A} and \mathcal{L} are the area and the perimeter of the billiard, and \mathcal{C} is a constant that carries information about the topological nature of the billiard. Strictly speaking, Weyl’s equation is only valid in the semiclassical limit, i.e., for large quantum numbers n ; however, it turns out that Eq. (5.3) holds well even in the lower part of the energy spectrum. For

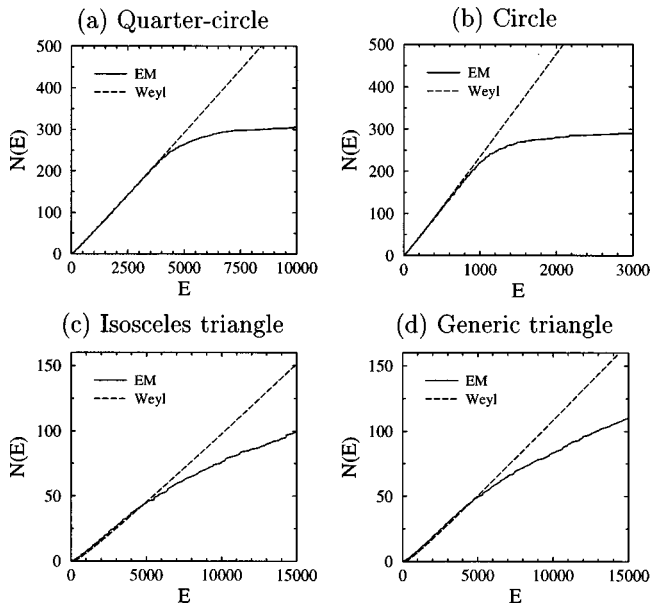


Fig. 8. Spectral staircase function $N(E)$.

a proper analysis of the energy level statistics, we first “unfold the spectrum”⁹ by linearly scaling the set of energies such that for the resulting sequence the mean level spacing is uniform, and equal to one, everywhere in the studied interval of the energy spectrum. This transformation is achieved by replacing the original set of energies E_n by $\tilde{E}_n = \langle N(E_n) \rangle$. To this end, we evaluate first the area \mathcal{A} and the perimeter \mathcal{L} of the billiard and, for the sake of simplicity, we neglect the constant \mathcal{C} in Eq. (5.3). The resulting staircase function $N(E)$ for the first 400 energy levels of the quarter- and full-circle billiards are given in Fig. 8(a) and (b). The agreement between our results and the corresponding Weyl formula is satisfactory only for the lowest 200 energy levels; only the values of these levels can be trusted and used for statistical analysis of the energy spectrum. Next we unfold the spectrum formed by the lowest 200 energies E_n , i.e., we evaluate Eq. (5.3) for each E_n in order to obtain the new energies \tilde{E}_n . For the first few energies this procedure is represented graphically in Fig. 9. Note that the integer part of \tilde{E}_n is about n and, as a result, the corresponding mean level spacing is characterized through $\langle s \rangle = \sum_{n=1}^N (\tilde{E}_{n+1} - \tilde{E}_n) / N \approx 1$. The resulting level spacing distributions $P(s)$ are shown in Fig. 10(a) and (b); for comparison $P_0(s)$ and $P_{\text{GOE}}(s)$ are also shown. As expected, $P(s)$ for both systems are best approximated by the Poisson distribution.

The staircase function $N(E)$ for the first 200 of 400 energy levels of the $\alpha_1 = \alpha_2 = 30^\circ$ isosceles triangle and the $\alpha_1 = 20^\circ$ and $\alpha_2 = 68^\circ$ generic-triangle billiards are given in Fig. 8(c) and (d). The agreement between $N(E)$ and the corresponding Weyl formula is acceptable only for the lowest fifty levels. For these levels the resulting $P(s)$ are shown in Fig. 10(c) and (d). As expected, $P(s)$ for the classically chaotic generic-triangle billiard is approximated by $P_{\text{GOE}}(s)$. Note, however, that $P(s)$ for the chaotic isosceles triangle seems to be different from both GOE or Poisson distributions. The deviation of $P(s)$ from a GOE distribution is due to the fact that the isosceles triangle has symmetry axes and, hence, has two sets of states, one for each symmetry class

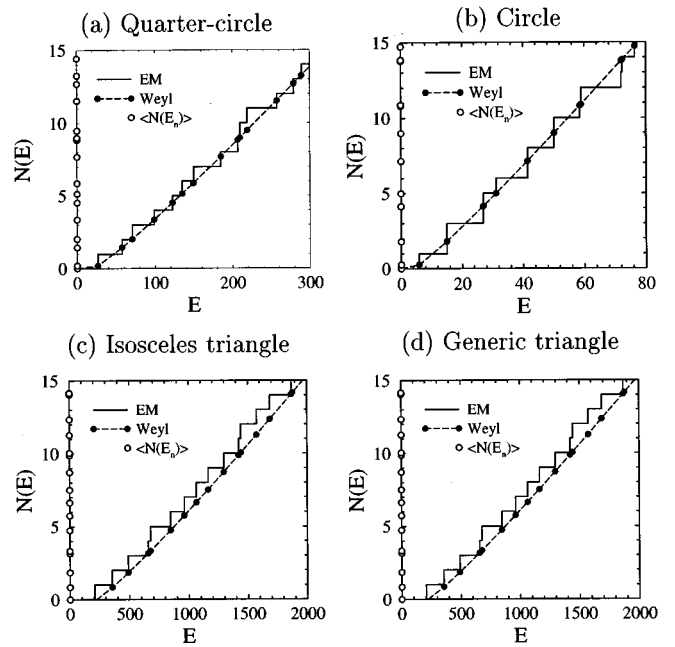


Fig. 9. Evaluation of $\tilde{E}_n = \langle N(E_n) \rangle$, i.e., “unfolding of the energy spectrum.” The open circles on the vertical axes represent the distribution of \tilde{E}_n 's on the new energy axis. The filled circles have coordinates (E_n, \tilde{E}_n) . At this scale, the discrepancy between the staircase function $N(E)$ and the Weyl formula $\langle N(E) \rangle$ is evident.

(even and odd reflection symmetry). As a result, $P(s)$ is best approximated with the superposition of two independent GOE distributions [see Fig. 10(c)], which describes the distribution for two independent sets of GOE distributed energy levels. A general expression for the level spacing distribution $P^{(N)}(s)$ corresponding to the superposition of N independent spectra with GOE statistics is given by⁹

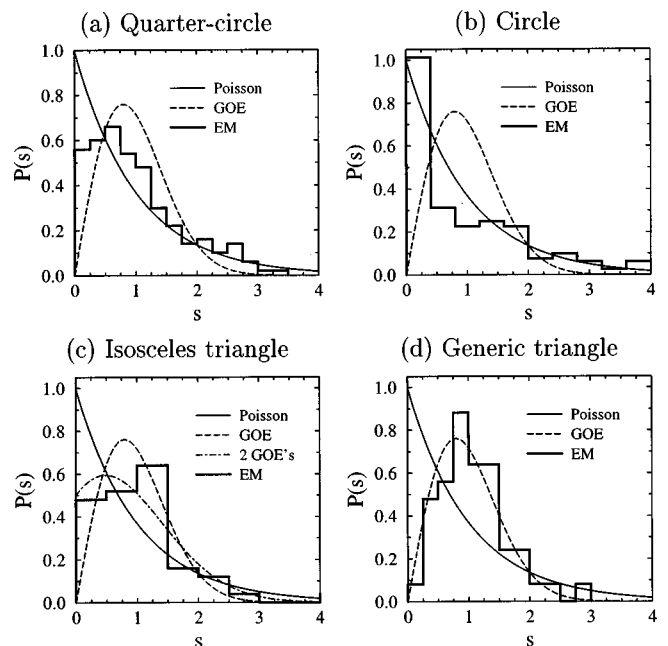


Fig. 10. Histogram of the energy level spacing distribution $P(s)$.

$$P^{(N)}(s) = \frac{\partial^2}{\partial s^2} \left[\operatorname{erfc} \left(\frac{\sqrt{\pi}}{2} \frac{s}{N} \right) \right]^N, \quad (5.4)$$

where $\operatorname{erfc}(z) = (2/\sqrt{\pi}) \int_z^\infty dt \exp(-t^2)$ is the complementary error function. Note that for $N=1$ one recovers Eq. (5.2), i.e., $P^{(1)}(s) = P_{\text{GOE}}(s)$, while in the limit $N \rightarrow \infty$ one recovers the Poisson distribution (5.1), i.e., $P^{(\infty)}(s) = P_0(s)$. For the isosceles triangle the appropriate level spacing distribution function is $P^{(2)}(s)$.

VI. CONCLUSIONS

In this paper we have presented a simple numerical method, the expansion method (EM), for calculating the stationary states, i.e., the energy spectrum and the corresponding wave functions, for quantum billiards. This method is conceptually simple and, accompanied by its computer implementation, e.g., as a MATHEMATICA notebook,⁷ it is most suitable for the investigation of quantum billiards in an introductory quantum mechanics course. To demonstrate the viability of the EM we have tested it with good results in the cases of quarter-, full-circle, and equilateral-triangle billiards where analytical results are available. Then, we have applied the EM to calculate the stationary states of nonintegrable (chaotic) triangle billiards which cannot be solved analytically. By using the energy spectra obtained with the EM, we have shown that there is a qualitative difference between the statistics of the energy levels of an integrable and a classically chaotic system. The applications of the EM presented in this article have been provided as examples and by no means exhaust the possibility of using this method to explore the exciting world of quantum billiards.

ACKNOWLEDGMENTS

This work was supported by a National Science Foundation REU fellowship (D.L.K.), and in part by NSF Grant No. DMR 91-20000 (through STCS, I.K.), and by funds of the University of Illinois at Urbana-Champaign (K.S.).

^{a)}Corresponding author. Electronic mail: kschulte@ks.uiuc.edu

¹R. L. Liboff, *Introductory Quantum Mechanics* (Addison-Wesley, Reading, MA, 1998), 3rd ed.

²For a recent review of some quantum and classical aspects of the circle billiard see, e.g., R. W. Robinet, "Visualizing the solutions for the circular infinite well in quantum and classical mechanics," *Am. J. Phys.* **64**, 440–446 (1996).

³For an overview of nanoelectronics see, e.g., F. A. Buot, "Mesoscopic physics and nanoelectronics: Nanoscience and nanotechnology," *Phys. Rep.* **234**, 73–174 (1993).

⁴M. C. Gutzwiller, *Chaos in Classical and Quantum Mechanics* (Springer, New York, 1990).

⁵For an introduction to the physics of classical billiard systems see, e.g., M. V. Berry, "Regularity and chaos in classical mechanics, illustrated by three deformations of a circular 'billiard,'" *Eur. J. Phys.* **2**, 91–102 (1981).

⁶A. Kudrolli, V. Kidambi, and S. Sridhar, "Experimental Studies of Chaos and Localization in Quantum Wave Functions," *Phys. Rev. Lett.* **75**, 822–825 (1995).

⁷The MATHEMATICA3.0 notebook which contains a complete numerical implementation of the EM is freely available from one of the authors (K.S.).

⁸M. L. Mehta, *Random Matrices* (Academic, Boston, 1990), 2nd ed.

⁹I. Kosztin and K. Schulten, "Boundary Integral Method for Stationary States of Two-Dimensional Quantum Systems," *Int. J. Mod. Phys. C* **8**, 293–325 (1997).

¹⁰M. V. Berry and M. Wilkinson, "Diabolical points in the spectra of triangles," *Proc. R. Soc. London, Ser. A* **392**, 15–43 (1984).

¹¹M. Tinkham, *Group Theory and Quantum Mechanics* (McGraw-Hill, New York, 1964).

SO WHAT?

One tries to discover some regularity, e.g., that the fault density is correlated with the ratio of the number of conduction electrons to atoms. Then one goes on to do it all again with another set of alloys. These papers did not effectively link with any other aspects of alloy theory or experiment. After a year or two of this, there is no longer any answer to the question: So what?? And when that point is reached, the paper is to be rejected by the editor, whatever the referee recommends. This seems straightforward enough; but one man's sense of pointlessness can be another man's experience of fascination. Furthermore, if one looks at a compilation such as a Landolt-Börnstein volume or a set of "critical" tables of melting-points, elastic moduli, etc., one comes to realize that most of the listed values come from small exercises in measuring, say, the melting-point of one of the thousands of new organic compounds discovered during a year. (This is, in part, why chemists' publications lists can be so enormous). Thus the question, so what?, as well as being important to save squandered journal space, is singularly difficult to resolve.

Robert W. Cahn, in *Editing the Refereed Scientific Journal*, edited by Robert A. Weeks and Donald L. Kinser (IEEE Press, New York, 1994), p. 38.